Oxygen reduction catalysis of Mn–Co spinel oxides on a graphite electrode in alkaline solution

Michio Sugawara,* Masamichi Ohno and Kenzo Matsuki

Department of Materials Science and Engineering, Yamagata University, 4-3-16 Yonezawa, Yamagata 992, Japan

Binary Mn–Co spinel oxides have been applied as catalysts for oxygen reduction on graphite electrodes in alkaline solution. Oxides with cation deficiencies were obtained by heating the homogeneous citrate and carbonate precursors with different atomic ratios of Mn/Co (0–1.5) at 400–600 °C in an O_2 atmosphere. The oxygen reduction was studied by a rotating ring-disk electrode method, and these oxides loaded onto graphite showed catalytic activity for the direct four-electron reduction of oxygen. It is considered that cation deficiencies in the oxide catalysts contribute to the appearance of catalytic activity.

A variety of transition-metal oxides have been applied as oxygen reduction catalysts on graphite electrodes and our group has reported this reaction with manganese oxide catalysts.[1–4] The catalytic reduction of oxygen on a spinel cobalt oxide (Co_3O_4) loaded electrode has also been reported.[5,6] This spinel oxide is easily prepared by heating cobalt salts, and mixed spinel oxides with stoichiometric composition (ACo_2O_4, A = transition-metal ion) are also well known.

On the other hand, when manganese, a transition-metal ion capable of adopting several oxidation states, is selected, it has been reported that the appropriate homogeneous precursors with different atomic ratios of Mn/Co crystallize into the spinel oxide with cation deficiencies upon heating.[7] Such spinel oxides are expected to show catalytic activity for oxygen reduction on graphite. In this paper, the preparation and characterization of such oxides are briefly described, and results on oxygen electrocatalysis discussed.

Experimental

Materials and characterization

All chemicals were reagent grade and used without further purification. The Mn–Co oxides were prepared by heating the citrate[8,9] or carbonate[7,10] precursors with an atomic ratio (Mn/Co) of 0–1.5 at 400 and 600 °C in an O_2 atmosphere. The resulting oxides were characterized by XRD, and specific surface area and electronic conductivity measurements. The XRD patterns were collected on a Simazu XD-D1 diffractometer with graphite monochromatized Cu-Kα radiation. The surface areas of oxide powders were measured according to the BET (single-point) method by N_2 physisorption at 77 K using a Micromeritics 2200-01 instrument. Conductivity measurements of the powdered oxides were carried out at a pressure of 1.50×10^7 N m^{-2} using the standard two-probe technique.

With $Mn_{3x}Co_{3-3x}O_4$ representing the formula of these oxides, the average oxidation number of M (M : Mn_xCo_{1-x}) was determined to calculate the O/M ratio by chemical analyses. A 50 mg sample of the oxide was dissolved in 10 ml of 0.1 mol dm^{-3} $FeSO_4$ acidified with 2 mol dm^{-3} H_2SO_4. The excess of unoxidized Fe^{2+} was then titrated with a standard 0.05 mol dm^{-3} $KMnO_4$ solution under nitrogen. The accuracy for the values of O/M ratios was better than ± 0.003.

Electrochemical measurements

A rotating ring-disk electrode (RRDE) method was applied for cathodic oxygen reduction catalysis. A mixture of the oxide and graphite (Lonza, KS44) with a weight ratio of 10 : 90 was thoroughly kneaded with small amount of paraffin to pack within the cavity of the gold disk, and used as the disk electrode. The value of collection efficiency (N) estimated from the arrangement of the gold ring and disk electrodes was 0.388. The counter and reference electrodes were platinum wire and 1 mol dm^{-3} NaOH/HgO/Hg, respectively.

The electrolyte was a 1 mol dm^{-3} NaOH solution saturated with oxygen and measurements were carried out at room temperature. The ring potential was kept at 100 mV corresponding to the oxidation of H_2O_2 to O_2, to detect the intermediate H_2O_2 in oxygen reduction, during the measurement of polarization curves on the disk electrode at a sweep rate of 5 mV s^{-1}.

Results and Discussion

Characterization of oxides

Fig. 1 shows XRD patterns of the oxides prepared by heating carbonate precursors with various Mn/Co atomic ratios at 400 and 600 °C. As reported by Jimenez-Mateos *et al.*, the

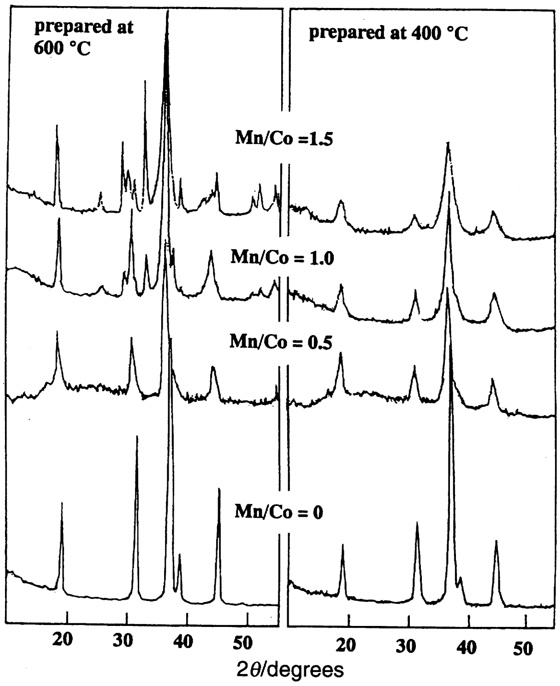

Fig. 1 XRD patterns of Mn–Co oxides prepared by heating the citrate precursor with different Mn/Co atomic ratios at 400 and 600 °C

products are crystallized into cubic spinel at Mn/Co atomic ratios of 0 and 0.5, and into tetragonal spinels at atomic ratios of 1.0 and 1.5, respectively. No significant difference in XRD patterns was observed for the oxides prepared by citrate and carbonate processes. The line broadening of the XRD peaks in the oxides with Mn/Co$\geqslant$0.5 shows a slight decrease in crystallinity.

Physicochemical properties are summarized in Table 1. The conductivity of the oxide powders was of the order of 10^{-5} to 10^{-6} S cm^{-1}, and showed semiconductor characteristics for each Mn/Co atomic ratio. The BET surface areas were relatively large especially for the oxides prepared from the carbonates at 400 °C. Oxides with larger surface areas may be preferable in applications for catalysts, and these preparation methods are therefore recommended over the usual ceramic route.

The positive deviation from a stoichiometrical O/M ratio of 1.333 indicates the presence of cation deficiency (except for the oxides with an Mn/Co atomic ratio of 0). There is no significant difference in the degree of deficiency between oxides prepared at 400 and 600 °C. The O/M ratios are fairly large for oxides with Mn/Co = 1.0 and 1.5, and values of > 1.5 are obtained in some cases.

The cation deficiency leads to an increase in the relative ratio of higher valent metal ions in the oxide. When the Mn/Co atomic ratio is 1.5, the average oxidation number of M is 3. This means that Mn^{4+} ion is necessarily present in the Mn–Co spinel oxides at O/M$\geqslant$1.5. Manganese ions tend to exhibit higher oxidation states (Mn^{3+} and Mn^{4+}) in an oxidizing atmosphere; it is therefore considered that modification with manganese ions would lead to cation deficiency when heated to crystallize into the spinel structure.

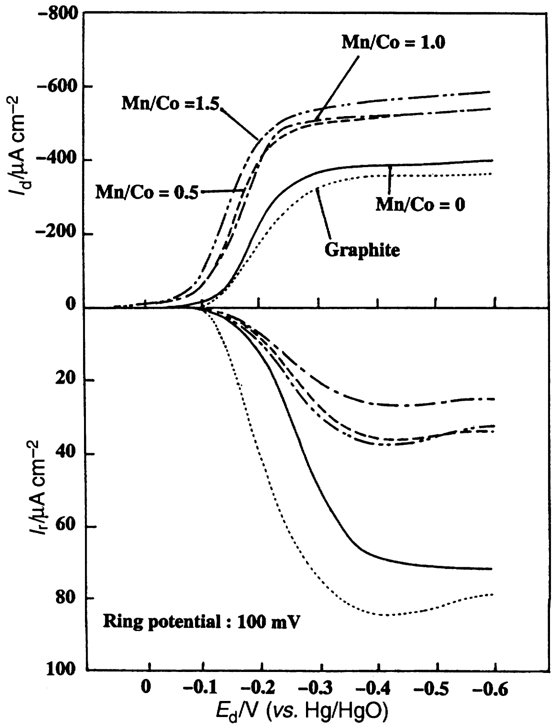

Fig. 2 Disk potential (E_d) *vs.* disk current (I_d) and ring current (I_r) plots in O_2 saturated 1 mol dm^{-3} NaOH at a rotating rate of 1000 rpm; disk potential sweep rate of 10 mV s^{-1}, graphite and Mn–Co oxide loaded graphites as disk electrodes

Oxygen reduction catalysis

Fig. 2 shows typical polarization curves of a graphite electrode loaded with oxides prepared by the citrate process at 400 °C. The disk current arising from oxygen reduction is increased and the ring current based on the reoxidation of intermediate hydrogen peroxide (HO_2^-) during oxygen reduction is decreased compared with a graphite electrode. This effect shows that oxide catalysts with Mn/Co > 0 enhance the catalytic activity of oxygen reduction.

It is generally accepted that oxygen reduction on graphite in alkaline solution proceeds to give HO_2^- by a two-electron transfer and that no further reduction of HO_2^- occurs. The ring current on graphite corresponds to the product of the collection efficiency (N) and the disk current. Accordingly, the decrease in the ring current on the oxide loaded electrode shows the four-electron reduction of oxygen or catalytic decomposition of HO_2^-. Furthermore, the disk current on the oxide loaded electrode starts to flow at potential 100 mV more negative than on graphite alone, while there is no effect of the catalyst on the potential at which the ring current starts to flow.

Oxygen reduction in alkaline solution is usually considered to proceed by two pathways; *viz.* direct four-electron reduction (k_1) and by series processes (k_2, k_3 and k_4), Scheme 1. A RRDE method is useful for the estimation of rate constants (k_1, k_2, k_3 and k_4) and has been applied for the study of oxygen reduction catalysis. The catalytic activity of Mn–Co oxides is also evaluated by the RRDE method in this discussion.[3,11]

When oxygen is reduced (first-order reaction for dissolved oxygen), eqn. (1)–(4) are found to hold. The B value obtained from the relationship between I_d^{-1} and $\omega^{-1/2}$ gives the number of electrons (n) transferred according to eqn. (2). Furthermore,

Table 1 Characterization of Mn–Co spinel oxides prepared by the citrate and carbonate processes

preparation method	preparation temp./°C	atomic ratio Mn/Co	conductivity/ S cm^{-1}	BET surface area/m^2 g^{-1}	O/M
citrate process	400	0	7.1×10^{-6}	9.6	1.326
		0.5	2.6×10^{-5}	35.2	1.430
		1.0	1.9×10^{-5}	81.2	1.528
		1.5	2.8×10^{-5}	66.7	1.490
	600	0	1.5×10^{-6}	7.9	1.338
		0.5	3.8×10^{-6}	15.0	1.401
		1.0	2.8×10^{-6}	27.8	1.453
		1.5	3.4×10^{-6}	10.6	1.484
carbonate process	400	0	2.6×10^{-5}	67.7	1.336
		0.5	9.7×10^{-5}	144.3	1.398
		1.0	8.8×10^{-5}	173.6	1.581
		1.5	1.6×10^{-5}	164.5	1.587
	600	0	5.3×10^{-5}	22.8	1.335
		0.5	7.1×10^{-5}	49.2	1.407
		1.0	4.9×10^{-5}	30.3	1.480
		1.5	1.6×10^{-5}	34.7	1.498

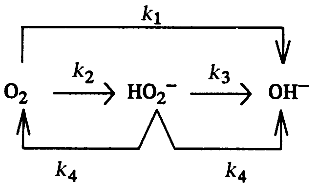

Scheme 1

the relationship between $(I_d/I_r)N$ and $\omega^{-1/2}$ based on eqn. (3) leads to the estimation of k_1/k_2 or (k_3+k_4).

$$1/I_d = 1/I_k + (1/B)\omega^{-1/2} \tag{1}$$

$$B = 0.62nFC_{O_2}D^{1/3}v^{-1/6}s(2\pi/60)^{1/2} \tag{3}$$

$$N(I_d/I_r) = 1 + 2k_1/k_2 + A + AM\omega^{-1/2} \tag{3}$$

$$A = \alpha\{(2k_1/k_1)(k_3+k_4) + (2k_3+k_4)\} \tag{4}$$

where I_d is the disk current, I_r the ring current, I_k the kinetic current, ω the electrode rotation rate, C_{O_2} the oxygen concentration, D the diffusion coefficient of oxygen, v the kinetic viscosity, s the electrode surface area, N the collection efficiency, and α and M are constants.

Fig. 3 and 4 show plots of I_d^{-1} and $(I_d/I_r)N$ *vs.* $\omega^{-1/2}$ for the polarization curves of the oxide (Mn/Co = 1.5) loaded graphite electrode, respectively. As shown in Fig. 3, the linear relationship, regardless of potential, indicates that the oxygen reduction on this electrode proceeds in a first-order manner. The intercept at $\omega^{-1/2}=0$ does not pass through the origin, and hence a kinetic current in addition to a simple diffusion controlled one is involved in the disk current. The reciprocal of the slope gives the value of B from which n can be calculated. The slopes shown in Fig. 4 are close to zero, and the ratio k_1/k_2 can be calculated from the intercept at $\omega^{-1/2}=0$. Results are obtained for oxides with a variety of Mn/Co ratios and are summarized in Table 2. The accuracies of the n and k_1/k_2 values calculated graphically were ±0.1 and ±0.3, respectively.

The graphite electrode generates HO_2^- by a two-electron transfer of O_2, and in the absence of further reduction or decomposition of HO_2^- in alkaline solution, $n=2$, as confirmed in the present study. As shown in Table 2, n values are >2 on the oxide loaded electrodes, and hence further reaction of HO_2^- takes place. Especially, oxides with Mn/Co > 0 show higher catalytic activity, apparent in the k_1/k_2 ratios. Since both k_3 and k_4 are negligibly small (Fig. 4), the enhancement of catalytic activity results from the occurrence of direct four-electron transfer of O_2 to OH^-. The contribution of this four-electron transfer becomes more significant in the oxides with Mn/Co > 0.5. The adsorption of intermediate HO_2^- should be taken into account to clarify in detail the reduction mechanisms,[12] in which the catalytic decomposition of HO_2^- (k_4) might be involved in the application for practical cells. Such processes seem to occur over timescales of less than the electrochemical measurements.

No significant difference in the k_1/k_2 ratio is observed with

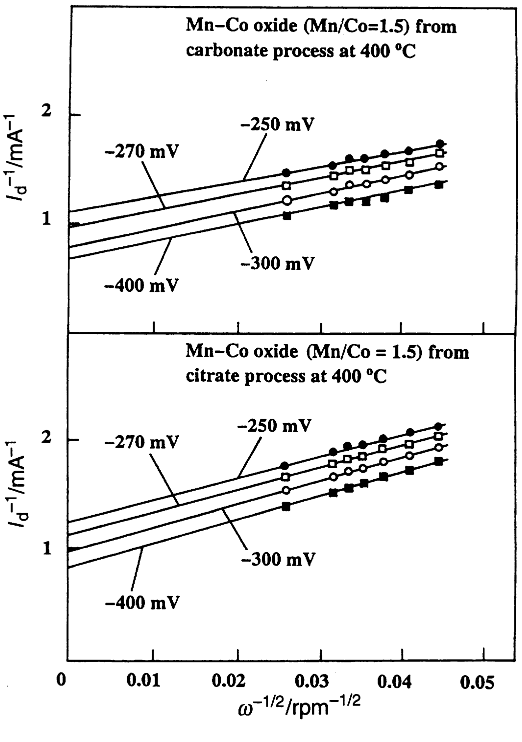

Fig. 3 I_d^{-1} *vs.* $\omega^{-1/2}$ plots at various disk potentials from the *E–I* curves measured using Mn–Co oxide (Mn/Co = 1.5) loaded graphite as the disk electrode

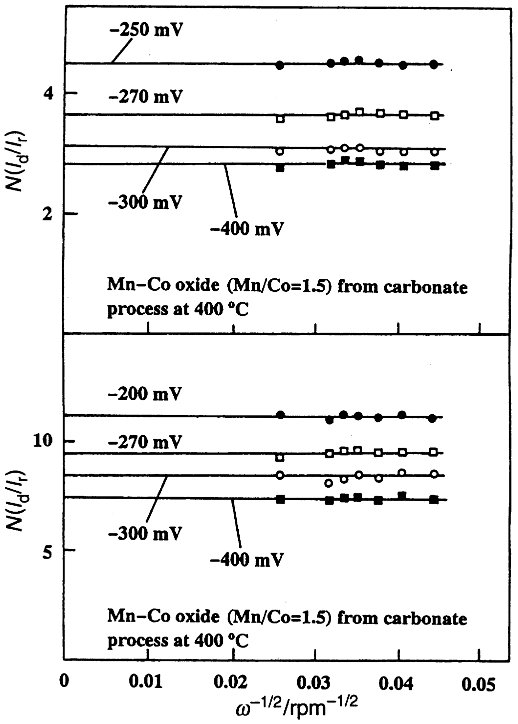

Fig. 4 $(I_d/I_r)N$ *vs.* $\omega^{-1/2}$ plots at various disk potentials from the *E–I* curves measured using Mn–Co oxide (Mn/Co = 1.5) loaded graphite as the disk electrode

Table 2 Some electrochemical characteristics of the oxide catalysts in oxygen reduction

preparation method	preparation temp./°C	Mn/Co	n	k_1/k_2[a]	O/M
citrate process	400	0	3.7	1.5	1.326
		0.5	4.0	3.1	1.430
		1.0	4.0	4.9	1.528
		1.5	4.0	2.9	1.490
	600	0	3.5	1.1	1.338
		0.5	4.0	4.8	1.382
		1.0	4.0	5.0	1.453
		1.5	4.0	7.1	1.484
carbonate process	400	0	3.6	1.3	1.336
		0.5	4.0	1.8	1.398
		1.0	4.0	4.2	1.581
		1.5	4.0	4.3	1.587
	600	0	3.6	1.6	1.335
		0.5	4.0	2.6	1.407
		1.0	4.0	4.4	1.480
		1.5	4.0	4.4	1.498

[a] At 400 mV.

different oxide preparation temperatures. Similarly, surface area differences do not appear to affect values of k_1/k_2, since oxygen reduction occurs on the smooth surface of the disk electrode prepared by kneading with paraffin. The effect of surface area on catalytic activity, however, may be expected when oxygen reduction proceeds on a gas diffusion electrode.

The catalytic activity and *n* values become low for stoichiometric Co_3O_4 compared with the cation deficient oxides with $Mn/Co > 0$, among which the oxides with $Mn/Co = 1.0$ and 1.5 are particularly effective oxygen reduction catalysts. It is considered that the catalytic activity may be correlated to the cation deficiency which is pronounced in the oxides with $Mn/Co = 1.0$ and 1.5. At present, we have no satisfactory explanations for the mechanism of the catalytic activity arising from cation deficient Mn–Co oxides, since no regular correlation was observed. However, eqn. (5) and (6) involving cation deficiencies may be presumed for four-electron transfer of O_2 into OH^-.

$$O_1^{2-} + 2\ V_M^{\bullet} + H_2O + 2e^- \rightarrow 2OH^- + V_O^x \qquad (5)$$

$$V_O^x + 1/2\ O_2 \rightarrow O_1^{2-} + 2\ V_M^{\bullet} \qquad (6)$$

(O_1^{2-} = lattice oxygen, $V_M^{\bullet}$ = cation deficiency, V_O^x = oxygen vacancy). Further studies are underway to investigate crystal structures of such cation deficient materials.

References

1 K. Matsuki, S. Mori and H. Kamata, *Denki Kagaku*, 1983, **51**, 691.
2 K. Matsuki, S. Mori and H. Kamata, *Denki Kagaku*, 1984, **52**, 129.
3 K. Matsuki and H. Kamata, *Electrochim. Acta*, 1986, **31**, 13.
4 M. Sugawara, M. Ohno and K. Matsuki, *Denki Kagaku*, 1992, **60**, 812.
5 J. R. Goldstein and A. C. C. Tseung, *J. Phys. Chem.*, 1972, **76**, 3646.
6 S. P. Jiang, Z. G. Lin and A. C. C. Tseung, *J. Electrochem. Soc.*, 1990, **137**, 759; 764.
7 J. M. Jimenez-Mateos, J. Morales and J. L. Trado, *J. Solid State Chem.*, 1989, **82**, 87.
8 M. Sugawara, M. Ohno and K. Matsuki, *Chem. Lett.*, 1991, 1465.
9 M. S. G. Baythoum and R. R. Sale, *J. Mater. Sci.*, 1982, **17**, 2757.
10 K. Vidyasagar, J. Gopalakrishnan and C. N. R. Rao, *Inorg. Chem.*, 1984, **23**, 1206.
11 M. R. Trasevih, A. Sadkowski and E. Yeager, *Comprehensive Treatise of Electrochemistry*, Plenum, New York, 1983, vol. 7, p. 301.
12 E. Yeager, *J. Electrochem. Soc.*, 1981, **128**, 160c.

Paper 6/07324G; *Received* 28*th October*, 1996